



HAL
open science

A coupled compressible two-phase flow with the biological dynamic modelling the anaerobic biodegradation process of waste in a landfill

Zakaria Belhachmi, Zoubida Mghazli, Salih Ouchtout

► To cite this version:

Zakaria Belhachmi, Zoubida Mghazli, Salih Ouchtout. A coupled compressible two-phase flow with the biological dynamic modelling the anaerobic biodegradation process of waste in a landfill. 2021. hal-03409786

HAL Id: hal-03409786

<https://hal.science/hal-03409786>

Preprint submitted on 30 Oct 2021

HAL is a multi-disciplinary open access archive for the deposit and dissemination of scientific research documents, whether they are published or not. The documents may come from teaching and research institutions in France or abroad, or from public or private research centers.

L'archive ouverte pluridisciplinaire **HAL**, est destinée au dépôt et à la diffusion de documents scientifiques de niveau recherche, publiés ou non, émanant des établissements d'enseignement et de recherche français ou étrangers, des laboratoires publics ou privés.

A coupled compressible two-phase flow with the biological dynamic modelling the anaerobic biodegradation process of waste in a landfill

Zakaria Belhachmi^{1,2}, Zoubida Mghazli³ and Salih Ouchtout^{1,3*}

¹ University of Haute-Alsace, IRIMAS UR 7499, F-68100 Mulhouse, France

² University of Strasbourg, France

³ Ibn Tofaïl University, Equipe d'Ingénierie Mathématique (EIMA), Laboratory: EDP, Algèbre et Géométrie Spectrale, Kénitra, Morocco

* **Correspondence:** salih.ouchtout@gmail.com

Abstract: In this article, we present and study a new coupled model combining the biological and the mechanical aspects describing respectively the process of the biogas production and the compressible two-phase leachate-biogas flow during the anaerobic biodegradation of organic matters in a landfill, considered as a reactive porous medium. The model obtained is governed by a reaction-diffusion system for the bacterial activity coupled with a compressible two-phase flow system of a non-homogeneous porous medium. We carry out the analysis and the numerical approximation of the model within a variational framework. We propose a full discrete system based on second order -BDF- time scheme and P1-conforming finite element and we derive an efficient algorithm for the coupled system. We perform some numerical simulations in 2D and 3D examples in agreement with the theoretical analysis.

Keywords: Anaerobic biodegradation, Compressible two-phase flow, Biogas production, Coupled model, Finite element method

1. Introduction

Waste management and renewable energy generation are two key issues in nowadays society. A major research field arising in recent years focuses on combining the two aforementioned topics by developing new techniques to handle waste and to use it in the energy production. The anaerobic digestion process is a natural biological process of the decomposition of the organic matter by microorganisms (bacteria) activated in the absence of oxygen. It consists of complex chemical reactions. In the long term, the organic matter is transformed into "biogas" which is a mixture of methane and carbon dioxide. The main steps of the degradation process are hydrolysis, acidogenesis, acetogenesis and methanogenesis, described in bio-mechanical models coupling PDE and ODE systems (see

[24, 27, 21, 14, 2, 35, 23, 40]). Most of these models are too complex, widely empirical, and not well suited for mathematical analysis and computations. An increasing research activity have emerged in the modelling to obtain accurate results in waste management but numerically tractable. We refer interested readers to [14, 17, 38, 18, 19, 36, 37, 16] and the references therein.

A bacterial dynamics model proposed by Bernard et al. [9], introduces a mere two step process that single out the dominant part in the bio-chemical transformations, namely, the acidogenesis using Monod's kinetics, and the methanogenesis using Haldane's kinetics. This approach, become now very popular in the field and constitutes our starting point in this paper (e.g. see [7, 6, 15, 4, 28, 24]).

Besides, the household waste landfill is a multi-phases medium consisting of solid, liquid and gas and considered as a non-homogeneous reactive porous medium. The altogether mechanical and biological dynamic is modelled with a coupled PDE-ODEs system describing the biodegradation process that produces a biogas and leachate (see [34], [1] and the references therein). This approach is widely followed in the field, particularly for the control and the optimization of the biogas production purposes. However, it has some limitations, mainly due to the omission of the non-homogeneous character of the porous medium and of the spatial distribution of the biological activity. In addition, influencing factors for accurate modelling, such as the role of humidity in the landfill are underrated within this approach.

In [7], the authors proposed a modification of the above approach to overcome partially such limitations by spatializing the biological activity, which is now governed by a diffusion PDEs system coupled to single phase flow (from Darcy flow equations).

In this article, we extend this novel approach to a two phases flow where the gaseous phase "biogas" is included in the model. The goal is to have a more accurate consideration of the mechanical aspects of the complex interaction between the medium and the biological activity in the landfill. The resulting mathematical model and its numerical approximation lead to a computation code in 2D and 3D which improve prediction tools and the waste degradation management.

The article is organised as follows : in Section 2. we introduce the coupled system of equations that consists of a unified model for the complex biological and mechanical interactions in the landfill. We firstly consider the standard ODEs system which describes the hydrolysis/acidogenesis and methanogenesis for the biogas production, under two specific growth rates [33]. In the spirit of [7], we transform the ODEs into a reaction-diffusion system of PDEs to spatialize the bacterial dynamic and to take into account the non-homogeneous distribution of methanogenesis bacteria which is a more realistic approach in a waste collection sites ([39], [32], [42]). Secondly, we give the full system governing the compressible two-phase leachate-biogas flow and the biodegradation.

We emphasise that the consideration of the spatial distribution acts as a regularization procedure for the initial ODEs system for which we have established in [33] the existence of several (stable and unstable) equilibria.

In Section 3., We consider the semi-discrete problems obtained with a second-order time scheme (BDF2) for the reaction-diffusion part and a semi-implicit Euler scheme for the two-phase flow equations. Section 4., is devoted to the full discrete system based on a standard P_1 -conforming finite elements method. In section 5., we present several 2D and 3D numerical results obtained by our computation code which is realized under the open source software FreeFem++ [25].

2. A coupled mathematical model for the biological dynamic and the flow

2.1. The bacterial dynamic: an anaerobic digestion system in two-step

The anaerobic digestion is a biological process that mineralizes organic substrates in the absence of the oxygen. The organic material is then transformed by microorganisms to a mixture (biogas) of methane (CH_4) and carbon dioxide (CO_2) through a complex reactions in parallel and/or in series. The modeling of this phenomena has been extensively studied over these last years and several mathematical models describing this process exist in the literature especially as a renewable energy (see [17] [31] [38] [8] [14] [3] and the references therein). The biogas production is a final step in the complex anaerobic digestion process called the methanogenesis.

The methane production process considered in this article is described as follows: a first step of hydrolysis / acidogenesis of the organic mater, represented by its concentration that we denote X , leads to the formation of the carbon dioxide (CO_2) and a simple soluble organic mater S . The latter is used as a substrate by methanogenic bacteria B which in turn produce the carbon dioxide (CO_2) as well as the methane (CH_4). At their death, the methanogenic bacteria in turn constitute a complex substrate to hydrolysis step (see FIGURE 1).

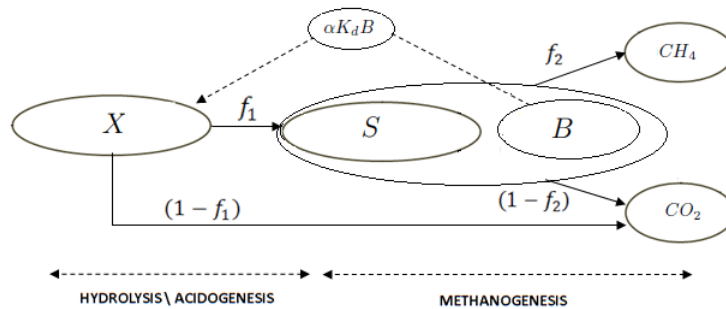


Figure 1. Scheme used for modeling anaerobic degradation of organic matter

The parameters f_1 and f_2 are the stoichiometric coefficients which represent the parts of organic matter (OM) transformed into simple OM or methane during the "hydrolysis / acidogenesis" step or methanogenesis step respectively. Consequently $(1 - f_1)$ and $(1 - f_2)$ represent the parts of OM transformed into CO_2 during these two steps respectively. K_d is the bacterial mortality rate and α is a constant $0 < \alpha \leq 1$ representing the fraction of the biomass mortality reused as a substrate in the methanogenesis. In what follows, we denote by K_h the rate of hydrolysis, Y the rate of use of the substrate and μ the specific growth rate.

Based on the principle of mass conservation and the law of bacterial growth, the model which describes the biological activity in this two step process for biogas production is given firstly by the system of ordinary differential equations (2.1), and in which the existence of several (stable and unsta-

ble) equilibria has been established (see [33]).

$$\left\{ \begin{array}{l} \frac{dX}{dt} = -K_h X + \alpha K_d B \\ \frac{dB}{dt} = (\mu(S) - K_d) B \\ \frac{dS}{dt} = f_1 K_h X - \frac{1}{Y} \mu(S) B \\ \frac{d[CO_2]}{dt} = (1 - f_1) K_h X + (1 - f_2) \frac{1 - Y}{Y} \mu(S) B \\ \frac{d[CH_4]}{dt} = f_2 \frac{1 - Y}{Y} \mu(S) B. \end{array} \right. \quad (2.1)$$

Next, we introduce the spatial diffusion (the spatial dependency of the bacterial dynamic), in order to consider the realistic case of nonhomogenous landfill, and to take into account some heterogeneities of the concentrations of microorganisms. This process was treated in the coupled model with the single phase leachate flow system (see [7]). We extend this novel approach to a two-phase flow where the gaseous phase, related to the biogas, is included in the model. The biodegradation model is then given as a reaction-diffusion system coupled with the flow system.

Let Ω be an open bounded subset of \mathbb{R}^d , $d \geq 2$, representing the landfill. We suppose that its boundary $\Gamma := \partial\Omega$ is Lipschitz-continuous and is the union of two parts Γ_D and Γ_N where Dirichlet and Neumann boundary conditions are respectively imposed, with $\Gamma_D \cap \Gamma_N = \emptyset$. The outward normal vector on Γ will be noted \mathbf{n} . We fix a time interval of biogas production $[0, T]$ where T corresponds to the moment when the leachate begins to stagnate at the bottom of the domain, or the moment when it is necessary to recover the biogas. Following the same approach as in [7], the biological activity can be modelled as follows:

$$(S1) \quad \left\{ \begin{array}{l} \frac{\partial \mathbf{U}}{\partial t} - \operatorname{div}(\overline{\overline{D}} \nabla \mathbf{U}) = \mathbf{F}^1(\mathbf{U}) \quad \text{in } \Omega \times]0, T[\\ \frac{d\mathbf{G}}{dt} = \mathbf{F}^2(\mathbf{U}) \quad \text{in } \Omega \times]0, T[\\ \overline{\overline{D}} \frac{\partial \mathbf{U}}{\partial n} = 0 \quad \text{on } \partial\Omega \times]0, T[\\ \mathbf{U}(0, \cdot) = \mathbf{U}^0(\cdot), \quad \mathbf{G}(0, \cdot) = \mathbf{G}^0(\cdot) \quad \text{in } \Omega, \end{array} \right. \quad (2.2)$$

where \mathbf{U} and \mathbf{G} are the dynamic variables of the system (2.2) defined as follows

$$\mathbf{U} = (u_1, u_2, u_3)^t = (X, B, S)^t, \quad \mathbf{G} = (u_4, u_5)^t = ([CO_2], [CH_4])^t \quad (2.3)$$

and $\overline{\overline{D}}$ is the diffusion coefficients matrix given as follows

$$\overline{\overline{D}} = \begin{pmatrix} D_1 & 0 & 0 \\ 0 & D_2 & 0 \\ 0 & 0 & D_3 \end{pmatrix},$$

where D_1 , D_2 and D_3 are, respectively, the diffusion coefficients of X , B and S .

The right-hand members \mathbf{F}^1 and \mathbf{F}^2 of the first and the second equation respectively in (2.2) are denoted by

$$\mathbf{F}^1(\mathbf{U}) = (F_1(U), F_2(U), F_3(U))^T, \quad \mathbf{F}^2(\mathbf{U}) = (F_4(U), F_5(U))^T. \quad (2.4)$$

and the functions F_i , $i = 1, 2, \dots, 5$ are defined as follows

$$\begin{aligned} F_1(\mathbf{U}) &= -K_h u_1 + \alpha K_d u_2, & F_2(\mathbf{U}) &= (\mu(u_3) - K_d) u_2, \\ F_3(\mathbf{U}) &= f_1 K_h u_1 - \frac{1}{Y} \mu(u_3) u_2, & F_5(\mathbf{U}) &= f_2 \frac{1-Y}{Y} \mu(u_3) u_2, \\ F_4(\mathbf{U}) &= (1 - f_1) K_h u_1 + (1 - f_2) \frac{1-Y}{Y} \mu(u_3) u_2. \end{aligned}$$

Several laws exist for the specific growth rate $\mu(S)$. The most used are the Monod law

$$\mu(S) = \frac{\mu_m S}{K_S + S} \quad (2.5)$$

and the Haldane law

$$\mu(S) = \frac{\mu_m S}{K_S + S + \frac{S^2}{K_I}} \quad (2.6)$$

where μ_m is the maximum growth rate, K_S is the half-saturation constant and K_I is the inhibition constant. The Monod law is related to saturation and limitation phenomena and the Haldane law is related to saturation and inhibition phenomena [9]. We note that the Monod function can be seen as a particular case of the Haldane function for large values of the parameter K_I .

Remark 1. We remark that the second equation of (2.2) can be written as follows

$$\frac{d\mathbf{G}}{dt} = \mathbf{F}^2(\mathbf{U}) = \begin{bmatrix} (1 - f_1) K_h u_1 + (1 - f_2) \frac{1-Y}{Y} \left(\frac{du_2}{dt} + K_d u_2 \right) \\ f_2 \frac{1-Y}{Y} \left(\frac{du_2}{dt} + K_d u_2 \right) \end{bmatrix}. \quad (2.7)$$

This remark will be used in the section 3.1 in order to linearize the system (2.2).

The system (2.2) allows us to compute the global rate of production of the biogas which constitutes the main part of the source/sink term in the next PDEs model of the flow in the waste.

2.2. Compressible two-phase leachate-biogas flow

The waste is considered as a porous medium consisting of a solid matrix, a liquid phase (leachate) and a gaseous phase formed by a binary mixture of methane and carbon dioxide (biogas). The modeling of a two-phase liquid-gas flow is based on a system of coupled equations (Darcy's law and the mass conservation equations) describing the flow of each phase simultaneously. In this context, we cite references [26, 13, 30, 20, 5, 29] for a detailed description of these equations. Based on these references, we are interested in the two-phase leachate-biogas flow.

The mass conservation equation for each of the phases, biogas and leachate, are given by

$$\frac{\partial(\rho_b\theta_b)}{\partial t} + \text{div}(\rho_b\mathbf{u}_b) = \alpha_b \quad (2.8)$$

$$\frac{\partial(\rho_l\theta_l)}{\partial t} + \text{div}(\rho_l\mathbf{u}_l) = \alpha_l \quad (2.9)$$

Where \mathbf{u}_i , ρ_i and θ_i are respectively the velocity, the density and the volume content of the fluid $i = b, l$. The indices b and l represent the biogas and leachate phases respectively. α_l and α_b are the source term of leachate and the rate of the biogas generation respectively and which will be given later. In what follows, we denote by ϕ the porosity of the medium.

The flow velocity for each phase, leachate and biogas, is governed by the generalized Darcy's law (low Reynolds number $Re < 1$):

$$\mathbf{u}_l = -K \frac{k_{rl}(\theta_l)}{\mu_l} (\nabla p_l - \rho_l g \mathbf{e}_z), \quad (2.10)$$

$$\mathbf{u}_b = -K \frac{k_{rb}(\theta_l)}{\mu_b} (\nabla p_b - \rho_b g \mathbf{e}_z). \quad (2.11)$$

where K , k_{rj} , p_j and μ_j are respectively the intrinsic permeability, the relative permeability, the pressure and the dynamic viscosity of phase j , for $j = l, b$. g is the modulus of the gravitational acceleration and $\mathbf{e}_z = \nabla z$ where z is the vertical axis directed downwards.

SOURCE TERMS

The anaerobic digestion process needs water for the production of biogas, so the source term of leachate α_l is related to the rate of the biogas generation α_b . We follow the approach of [7, 1, 3, 9]:

$$\alpha_l = -\gamma \alpha_b = -\gamma \tilde{g}(\omega) A_m C_{Tb} \lambda_{cin}, \quad (2.12)$$

where $\gamma = M_{H_2O}/(3.4 \times M_b)$ with M_{H_2O} and M_b are respectively the molar mass of H_2O and the biogas, \tilde{g} is an explicit function on the variable ω , the humidity rate defined by

$$\theta = \frac{\rho_0}{\rho} \omega$$

with ρ_0 the density of the dry medium, A_m is the biodegradable part of the waste, C_{Tb} is a positive constant and λ_{cin} is the rate of the biogas production (see [21] and [22]) :

$$\lambda_{cin} = \frac{dC_{biogaz}}{dt} = \frac{d([CH_4] + [CO_2])}{dt}. \quad (2.13)$$

Experimental studies (see [3], [22]) show that below a minimal value ω_{min} and above a maximum value ω_{max} there is no biogas production. The function \tilde{g} increases in $[\omega_{min}, \omega_1]$, is constant in $[\omega_1, \omega_2]$ and decreases in $[\omega_2, \omega_{max}]$ for some values ω_1 and ω_2 (see FIGURE 2).

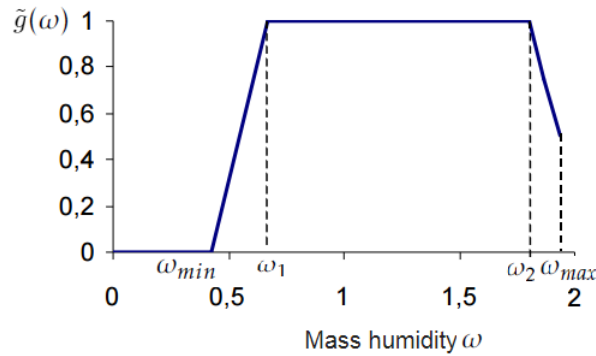


Figure 2. The empirical function $\tilde{g}(\omega)$.

The separation interface of the two fluids is characterized by an interfacial tension due to the effects of collision and adhesion between the two phases and so induces a pressure difference called capillary pressure:

$$p_c := p_b - p_l. \quad (2.14)$$

Capillary pressure and permeability depend on water content via different empirical models (see for example the models: Van Genuchten [41], Campbell [12] and Brooks-Corey [11]). We can find the parameter values of these model applied in biodegradation in the references [3, 31, 8]. We use here the Campbell model given as follows in the unsaturated porous medium case:

$$p_c(\theta_l) = p_{ce} \left(\frac{\theta_l}{\theta_s} \right)^{-b}, \quad \theta_l(p_c) = \theta_s \left(\frac{p_c}{p_{ce}} \right)^{-\frac{1}{b}} \quad (2.15)$$

$$k_{rl}(\theta_l) = \left(\frac{\theta_l}{\theta_s} \right)^B \quad \text{with} \quad B = 2b + 3 \quad (2.16)$$

$$k_{rb}(\theta_l) = \frac{\theta_l}{\theta_s} \left(1 - \frac{\theta_l}{\theta_s} \right)^2 \quad (2.17)$$

where θ_s is the saturation water content, p_{ce} is a scaling factor and b is a given parameter.

Changes of variables:

In what follows we will introduce, instead of the pressures, the heights in column. These quantities are defined by:

$$h_l : = \frac{p_l - p_0}{\rho_l g}, \quad (2.18)$$

$$h_b : = \frac{p_b - p_0}{\rho_l g}, \quad (2.19)$$

$$h_c : = h_b - h_l = \frac{p_c}{\rho_l g}, \quad (2.20)$$

where p_0 is the reference pressure, h_l (resp. h_b) represents the column height of leachate (resp. of biogas), and h_c the capillary height.

Taking into account these new variables, equations (2.10) and (2.11) become:

$$\mathbf{u}_l = -K \frac{k_{rl}(\theta_l)}{\mu_l} \rho_l g (\nabla h_l - \mathbf{e}_z), \quad (2.21)$$

$$\mathbf{u}_b = -K \frac{k_{rb}(\theta_l)}{\mu_b} \rho_l g (\nabla h_b - \frac{\rho_b}{\rho_l} \mathbf{e}_z). \quad (2.22)$$

In order to simplify the writing of these expressions, we note

$$k_l(\theta_l) : = K \frac{k_{rl}(\theta_l)}{\mu_l} \rho_l g, \quad (2.23)$$

$$k_b(\theta_l) : = K \frac{k_{rb}(\theta_l)}{\mu_b} \rho_l g, \quad (2.24)$$

k_l and k_b represent the hydraulic conductivity of leachate and biogas respectively.

Using (2.21) and (2.23) and taking into account that ρ_l is constant, equation (2.9) becomes:

$$\frac{\partial \theta_l}{\partial t} - \text{div}(k_l(\theta_l)(\nabla h_l - \mathbf{e}_z)) = \alpha_l \rho_l^{-1} \quad (2.25)$$

Next, we have

$$\frac{\partial \theta_l}{\partial t} = \frac{d\theta_l}{dh_c} \frac{\partial h_c}{\partial t} = C_l(h_c) \frac{\partial h_c}{\partial t} \quad (2.26)$$

where

$$C_l(h_c) = \frac{d\theta_l}{dh_c} \quad (2.27)$$

represents the capillary capacity. Using (2.20) and (2.23), the generalized darcy flow of leachate (2.21) becomes

$$\mathbf{u}_l = k_l(\theta_l)(\nabla h_c - \nabla h_b + \mathbf{e}_z), \quad (2.28)$$

and from (2.25) and (2.26), we get

$$C_l(h_c) \frac{\partial h_c}{\partial t} - \text{div}\left(k_l(\theta_l)(\nabla h_b - \nabla h_c - \mathbf{e}_z)\right) = \alpha_l \rho_l^{-1}. \quad (2.29)$$

The continuity equation of the biogas phase is (with the notation (2.24))

$$\frac{\partial(\rho_b \theta_b)}{\partial t} - \operatorname{div} \left(\rho_b k_b(\theta_l) (\nabla h_b - \frac{\rho_b}{\rho_l} \mathbf{e}_z) \right) = \alpha_b \quad (2.30)$$

which implies, since $\phi = \theta_l + \theta_b$

$$(\phi - \theta_l) \frac{\partial \rho_b(h_b)}{\partial t} + \rho_b(h_b) \frac{\partial(\phi - \theta_l)}{\partial t} - \operatorname{div} \left(\rho_b(h_b) k_b(\theta_l) (\nabla h_b - \frac{\rho_b}{\rho_l} \mathbf{e}_z) \right) = \alpha_b. \quad (2.31)$$

We assume that the compressibility of biogas obeys the ideal gas equation

$$\rho_b(h_b) = \rho_{0b} \left(\frac{p_b}{p_0} \right) \quad (2.32)$$

where p_0 and ρ_{0b} are respectively the pressure and the reference density.

Taking into account the relation (2.19), the equation (2.32) becomes

$$\rho_b = \rho_{0b} \left(1 + \frac{h_b}{h_0} \right) \quad (2.33)$$

where $h_0 = \frac{p_0}{\rho_l g}$, and this gives

$$(\phi - \theta_l) \frac{\rho_{0b}}{h_0} \frac{\partial h_b}{\partial t} - \rho_b(h_b) \frac{\partial \theta_l}{\partial t} - \operatorname{div} \left(\rho_b(h_b) k_b(\theta_l) (\nabla h_b - \frac{\rho_b}{\rho_l} \mathbf{e}_z) \right) = \alpha_b, \quad (2.34)$$

or

$$(\phi - \theta_l) \frac{\rho_{0b}}{h_0} \frac{\partial h_b}{\partial t} - \rho_b(h_b) C_l(h_c) \frac{\partial h_c}{\partial t} - \operatorname{div} \left(\rho_b(h_b) k_b(\theta_l) (\nabla h_b - \frac{\rho_b}{\rho_l} \mathbf{e}_z) \right) = \alpha_b. \quad (2.35)$$

We finally get the following system

$$\begin{cases} C_l(h_c) \frac{\partial h_c}{\partial t} + \operatorname{div}(\mathbf{u}_l) = \rho_l^{-1} \alpha_l, \\ \bar{k}_l(h_c) \mathbf{u}_l = \nabla h_c - \nabla h_b + \mathbf{e}_z, \\ A_1(h_c) \frac{\partial h_b}{\partial t} - A_2(h_c, h_b) \frac{\partial h_c}{\partial t} + \operatorname{div}(\rho_b(h_b) \mathbf{u}_b) = \alpha_b, \\ \bar{k}_b(h_c) \mathbf{u}_b = -\nabla h_b + c_1 h_b \mathbf{e}_z + c_2 \mathbf{e}_z, \end{cases} \quad (2.36)$$

which can also be written in the following form

$$\begin{cases} C_l(h_c) \frac{\partial h_c}{\partial t} - \operatorname{div} (k_l(\theta_l(h_c)) (\nabla h_b - \nabla h_c - \mathbf{e}_z)) = \alpha_l \rho_l^{-1}, \\ A_1(h_c) \frac{\partial h_b}{\partial t} - A_2(h_c, h_b) \frac{\partial h_c}{\partial t} \\ \quad - \operatorname{div} \left(\rho_b(h_b) k_b(\theta_l) \left(\nabla h_b - \frac{\rho_b(h_b)}{\rho_l} \mathbf{e}_z \right) \right) = \alpha_b. \end{cases} \quad (2.37)$$

where

$$\begin{aligned} A_1(h_c) &= \frac{(\phi - \theta_l(h_c))\rho_{0b}}{h_0}, \\ A_2(h_c, h_b) &= \rho_b(h_b)C_l(h_c), \\ \bar{k}_l(h_c) &= k_l(\theta_l(h_c))^{-1} \\ \bar{k}_b(h_c) &= k_b(\theta_l(h_c))^{-1} \\ c_1 &= \frac{\rho_{0b}}{\rho_l h_0}, \quad c_2 = \frac{\rho_{0b}}{\rho_l}, \end{aligned}$$

Boundary and initial conditions

To complete the equations of the compressible two-phase flow system (2.36), we consider the following boundary and initial conditions.

At $t = 0$, the initial conditions on the column heights in h_b and h_c are given by

$$h_c(0, x) = h_{c,0}(x), \quad x \in \Omega, \quad (2.38)$$

$$h_b(0, x) = h_{b,0}(x), \quad x \in \Omega. \quad (2.39)$$

We assume that, at the surface of the domain Γ_D , the contact with the atmosphere imposes Dirichlet-type conditions on the column heights of h_b and h_c . The limiting conditions on Γ_D are thus given by

$$h_c = h_{c,D} \quad \text{on } \Gamma_D \times]0, T[, \quad (2.40)$$

$$h_b = h_{b,D} \quad \text{on } \Gamma_D \times]0, T[. \quad (2.41)$$

We assume that the walls and the bottom of the domain are impermeable. These situations are represented by the following homogeneous Neumann conditions

$$k_l(\theta_l(h_c))(\nabla h_b - \nabla h_c - \mathbf{e}_z) \cdot \mathbf{n} = \mathbf{v}_l = 0 \quad \text{on } \Gamma_N \times]0, T[, \quad (2.42)$$

$$k_b(\theta_l(h_c))(\nabla h_b - \frac{\rho_b}{\rho_l} \mathbf{e}_z) \cdot \mathbf{n} = \mathbf{v}_b = 0 \quad \text{on } \Gamma_N \times]0, T[. \quad (2.43)$$

Consequently, equations (2.37) together with boundary and initial conditions, give the following sys-

tem

$$\begin{aligned}
 (S2) \left\{ \begin{aligned}
 & C_l(h_c) \frac{\partial h_c}{\partial t} - \operatorname{div} (k_l(\theta_l(h_c))(\nabla h_b - \nabla h_c - \mathbf{e}_z)) = \alpha_l \rho_l^{-1} \\
 & \hspace{15em} \text{in } \Omega \times]0, T[, \\
 & A_1(h_c) \frac{\partial h_b}{\partial t} - A_2(h_c, h_b) \frac{\partial h_c}{\partial t} - \operatorname{div} (\rho_b(h_b) k_b(\theta_l)(\nabla h_b - \frac{\rho_b(h_b)}{\rho_l} \mathbf{e}_z)) = \alpha_b \\
 & \hspace{15em} \text{in } \Omega \times]0, T[, \\
 & h_l = h_{l,D} \text{ and } h_b = h_{b,D} \\
 & \hspace{10em} \text{on } \Gamma_D \times]0, T[, \\
 & k_l(\theta_l(h_c))(\nabla h_b - \nabla h_c - \mathbf{e}_z) \cdot \mathbf{n} = 0 \text{ and } k_b(\theta_l(h_c))(\nabla h_b - \frac{\rho_b}{\rho_l} \mathbf{e}_z) \cdot \mathbf{n} = 0 \\
 & \hspace{15em} \text{on } \Gamma_N \times]0, T[, \\
 & h_c(0, x) = h_{c,0}(x) \text{ and } h_b(0, x) = h_{b,0}(x) \\
 & \hspace{15em} \text{in } \Omega
 \end{aligned} \right. \tag{2.44}
 \end{aligned}$$

2.3. The final Model

The final mathematical model describing both the degradation of the organic mater and the compressible two-phase leachate-biogas during the anaerobic digestion process for biogas production is given by the system (2.2)=(S1) and the system (2.44)=(S2).

3. Variational formulation and semi-discrete system

In what follows, We make some assumptions.

Hypothesis 1. *The coefficients α , K_d , Y , f_1 and f_2 fulfill the following conditions.*

1. *The proportion of nutrient recycling α cannot exceed 1*

$$0 < \alpha \leq 1. \tag{3.1}$$

2. *The mortality rate K_d is a positive parameter which is below the maximum growth rate*

$$0 < K_d < \max_s \mu(s). \tag{3.2}$$

3. *The rate of use of the substrate is a strictly positive parameter such that*

$$0 < Y < 1. \tag{3.3}$$

4. *The stoichiometric coefficients parameters f_1 and f_2 are strictly positive and satisfy*

$$0 < f_1 < 1 \text{ and } 0 < f_2 < 1. \tag{3.4}$$

The final model obtained in (2.2) and (2.44) is weakly coupled, therefore, we can separate the analysis of the system (2.2) and the system (2.44).

Due to the fact that the specific growth rate $\mu(\cdot)$ is a nonnegative and bounded function in both Monod and Haldane cases, and all the constants K_h, K_d, f_1, f_2 and Y lie in $]0, 1[$, it is readily checked that assumptions of Theorem 1 in [10] are verified and we have the existence and the uniqueness of the solution of the system (2.2) (see [7]). We can also find a theorem of existence and uniqueness for the corresponding incompressible two-phase flow system in [20].

3.1. Semi-discretization in time and variational formulation of the system (S1)

Let $\tau_n = t^{n+1} - t^n$, $n = 0, \dots, N$, where $N \in \mathbb{N}^*$, be a partition of $[0, T]$ with $t^0 = 0$ and $t^N = T$. In what follows we denote by f^n the values of a function f at the time t_n .

The semi-discrete scheme for the system (S1) considered here is the second order backward differentiation formula BDF2 for the variables (X, S, B) and the implicit Euler scheme for the ODE on $([CO_2], [CH_4])$. The problem reads: find $\mathbf{U}^{n+1} \in Z = (H^1(\Omega))^3$ such that

$$\int_{\Omega} \frac{3\mathbf{U}^{n+1} - 4\mathbf{U}^n + \mathbf{U}^{n-1}}{2\tau_n} \cdot \mathbf{v} dx + \int_{\Omega} \overline{\overline{D}} \nabla \mathbf{U}^{n+1} \cdot \nabla \mathbf{v} dx = \int_{\Omega} \mathbf{F}^1(\mathbf{U}^{n+1}) \cdot \mathbf{v} dx \quad \forall \mathbf{v} \in Z, \quad (3.5)$$

where the initial values are computed as follow: find $\mathbf{U}^1 \in Z$ such that

$$\int_{\Omega} \frac{\mathbf{U}^1 - \mathbf{U}^0}{\tau_0} \cdot \mathbf{v} dx + \int_{\Omega} \overline{\overline{D}} \nabla \mathbf{U}^1 \cdot \nabla \mathbf{v} dx = \int_{\Omega} \mathbf{F}^1(\mathbf{U}^1) \cdot \mathbf{v} dx \quad \forall \mathbf{v} \in Z, \quad (3.6)$$

and where the notation $\nabla \mathbf{U} \cdot \nabla \mathbf{v}$ means the vector with the components $\nabla U_i \cdot \nabla v_i$, for $i = 1, 2, 3$.

We linearize the scheme by using the Taylor formula

$$\mathbf{F}^1(\mathbf{U}^{n+1}) \simeq \mathbf{F}^1(\mathbf{U}^n) + J_{\mathbf{F}^1}(\mathbf{U}^n)(\mathbf{U}^{n+1} - \mathbf{U}^n) \quad (3.7)$$

where $J_{\mathbf{F}^1}$ is the Jacobian matrix of the vector function \mathbf{F}^1 . Consequently, the final BDF2 scheme reads : find $\mathbf{U}^1 \in Z = (H^1(\Omega))^3$ such that

$$\int_{\Omega} [\tau_0^{-1} \mathbf{I}_3 - J_{\mathbf{F}^1}(\mathbf{U}^0)] \mathbf{U}^1 \cdot \mathbf{v} dx + \int_{\Omega} \overline{\overline{D}} \nabla \mathbf{U}^1 \cdot \nabla \mathbf{v} dx = \int_{\Omega} [\tau_0^{-1} \mathbf{U}^0 + \mathbf{F}^1(\mathbf{U}^0) - J_{\mathbf{F}^1}(\mathbf{U}^0) \mathbf{U}^0] \cdot \mathbf{v} dx \quad \forall \mathbf{v} \in Z, \quad (3.8)$$

and for all $n \geq 1$, find $\mathbf{U}^{n+1} \in Z$ such that

$$\begin{aligned} & \int_{\Omega} \left[\frac{3}{2\tau_n} \mathbf{I}_3 - J_{\mathbf{F}^1}(\mathbf{U}^n) \right] \mathbf{U}^{n+1} \cdot \mathbf{v} dx + \int_{\Omega} \overline{\overline{D}} \nabla \mathbf{U}^{n+1} \cdot \nabla \mathbf{v} dx = \\ & \int_{\Omega} \left[\frac{4\mathbf{U}^n - \mathbf{U}^{n-1}}{2\tau_n} + \mathbf{F}^1(\mathbf{U}^n) - J_{\mathbf{F}^1}(\mathbf{U}^n) \mathbf{U}^n \right] \cdot \mathbf{v} dx \quad \forall \mathbf{v} \in Z. \end{aligned} \quad (3.9)$$

On the other hand, by using the Remark 1, the approximation of \mathbf{G} at $t = t_{m+1}$ $\mathbf{G}^{m+1} = (u_4^{m+1}, u_5^{m+1})^T$, for $0 \leq m \leq n$, is given by

$$\frac{u_4^{m+1} - u_4^m}{\tau_m} = (1 - f_1) K_h u_1^{m+1} + (1 - f_2) \frac{1 - Y}{Y} \left(\frac{u_2^{m+1} - u_2^m}{\tau_m} + K_d u_2^{m+1} \right), \quad (3.10)$$

$$\frac{u_5^{m+1} - u_5^m}{\tau_m} = f_2 \frac{1 - Y}{Y} \left(\frac{u_2^{m+1} - u_2^m}{\tau_m} + K_d u_2^{m+1} \right). \quad (3.11)$$

3.2. Semi-discretization in time and variational formulation of (S2)

The semi discretization in time and linearization of the flow system (S2) is realized in the implicit scheme and is written as follow

$$C_l(h_c^n) \frac{h_c^{n+1} - h_c^n}{\tau_n} - \operatorname{div} \left(k_l(h_c^n) (\nabla h_b^{n+1} - \nabla h_c^{n+1} - \mathbf{e}_z) \right) = \rho_l^{-1} \alpha_l^{n+1} \quad \text{in } \Omega, \quad (3.12)$$

$$\begin{aligned} A_1(h_c^n) \frac{h_b^{n+1} - h_b^n}{\tau_n} - A_2(h_c^n, h_b^n) \frac{h_c^{n+1} - h_c^n}{\tau_n} \\ - \operatorname{div} \left(\rho_b(h_b^n) k_b(h_c^n) (\nabla h_b^{n+1} - \frac{\rho_b(h_b^n)}{\rho_l} \mathbf{e}_z) \right) = \alpha_b^{n+1} \quad \text{in } \Omega, \end{aligned} \quad (3.13)$$

where the unknowns h_c^{n+1} and h_b^{n+1} are the approximations of $h_c(t_{n+1})$ and $h_b(t_{n+1})$ such that the initial conditions are $h_c(0, x) = h_{c,0}(x)$ and $h_b(0, x) = h_{b,0}(x)$ in Ω and the boundary conditions are

$$h_c^{n+1} = h_{c,D} \quad \text{and} \quad h_b^{n+1} = h_{b,D} \quad \text{on } \Gamma_D, \quad (3.14)$$

$$k_l(h_c^n) (\nabla h_b^{n+1} - \nabla h_c^{n+1} - \mathbf{e}_z) \cdot \mathbf{n} = 0 \quad \text{on } \Gamma_N, \quad (3.15)$$

$$k_b(h_c^n) (\nabla h_b^{n+1} - \frac{\rho_b(h_b^n)}{\rho_l} \mathbf{e}_z) \cdot \mathbf{n} = 0 \quad \text{on } \Gamma_N. \quad (3.16)$$

We introduce the following functional space

$$H_1 = \left\{ \mathbf{v} \in H^1(\Omega), \quad \mathbf{v} = 0 \text{ on } \Gamma_D \right\}, \quad (3.17)$$

The weak formulation of (3.12)-(3.13) with the conditions (3.14)-(3.16) is written as follows:

$$\left\{ \begin{array}{l} \text{Find } h_c^{n+1} \in h_{c,D} + H_1 \text{ and } h_b^{n+1} \in h_{b,D} + H_1 \text{ such that} \\ \int_{\Omega} C_l(h_c^n) \frac{h_c^{n+1}}{\tau_n} \psi dx + \int_{\Omega} k_l(h_c^n) (\nabla h_b^{n+1} - \nabla h_c^{n+1} - \mathbf{e}_z) \cdot \nabla \psi dx \\ \quad = \int_{\Omega} \rho^{-1} \alpha_l^{n+1} \psi dx + \int_{\Omega} C_l(h_c^n) \frac{h_c^n}{\tau_n} \psi dx, \quad \forall \psi \in H^1(\Omega) \\ \int_{\Omega} A_1(h_c^n) \frac{h_b^{n+1}}{\tau_n} \varphi dx - \int_{\Omega} A_2(h_c^n, h_b^n) \frac{h_c^{n+1}}{\tau_n} \varphi dx \\ \quad + \int_{\Omega} \rho_b(h_b^n) k_b(h_c^n) (\nabla h_b^{n+1} - \frac{\rho_b(h_b^n)}{\rho_l} \mathbf{e}_z) \cdot \nabla \varphi dx = \int_{\Omega} \alpha_b^{n+1} \varphi dx \\ \quad + \int_{\Omega} A_1(h_c^n) \frac{h_b^n}{\tau_n} \varphi dx + \int_{\Omega} A_2(h_c^n, h_b^n) \frac{h_c^n}{\tau_n} \varphi dx, \quad \forall \varphi \in H^1(\Omega) \end{array} \right. \quad (3.18)$$

4. Discrete problem

We assume in this section that Ω is a polygon domain of \mathbb{R}^d . Let \mathcal{T}_h be a partition of $\bar{\Omega}$ into triangles T (in \mathbb{R}^2) or tetrahedra T (in \mathbb{R}^3) and we denote by $P_k(O)$ the space of polynomial functions defined in a subset O of \mathbb{R}^d of total degree at most k . In order to define the full discretization of the problem (2.2),(2.44), we introduce the following finite-dimensional functional spaces:

$$Z_h = \left\{ \mathbf{v}_h \in (C(\bar{\Omega}))^3 ; \forall T \in \mathcal{T}_h \quad \mathbf{v}_h|_T \in (P_1(T))^3 \right\}, \quad (4.1)$$

$$H_{0,h} = \left\{ \mathbf{v}_h \in C(\bar{\Omega}) ; \forall T \in \mathcal{T}_h \quad \mathbf{v}_h|_T \in P_1(T) \right\}, \quad (4.2)$$

and

$$H_{1,h} = \left\{ \mathbf{v}_h \in C(\bar{\Omega}) ; \forall T \in \mathcal{T}_h \quad \mathbf{v}_h|_T \in P_1(T), \quad \mathbf{v}_h|_{\Gamma_D} = 0 \right\}. \quad (4.3)$$

4.1. Full discretization of the system (SI)

We discretize the equations (3.8)-(3.11) via the finite element method in the finite dimensional space Z_h . The problem consists to find $\mathbf{U}_h^1 \in Z_h$ such that

$$\begin{aligned} \int_{\Omega} \left[\tau_0^{-1} \mathbf{I}_3 - J_{\mathbf{F}^1}(\mathbf{U}^0) \right] \mathbf{U}_h^1 \cdot \mathbf{v} dx + \int_{\Omega} \bar{\bar{D}} \nabla \mathbf{U}_h^1 \cdot \nabla \mathbf{v} dx = \\ \int_{\Omega} \left[\tau_0^{-1} \mathbf{U}^0 + \mathbf{F}^1(\mathbf{U}^0) - J_{\mathbf{F}^1}(\mathbf{U}^0) \mathbf{U}^0 \right] \cdot \mathbf{v} dx \quad \forall \mathbf{v} \in Z_h, \end{aligned} \quad (4.4)$$

and for all $n \geq 1$, find $\mathbf{U}_h^{n+1} \in Z_h$ such that

$$\begin{aligned} \int_{\Omega} \left[\frac{3}{2\tau_n} \mathbf{I}_3 - J_{\mathbf{F}^1}(\mathbf{U}_h^n) \right] \mathbf{U}_h^{n+1} \cdot \mathbf{v} dx + \int_{\Omega} \overline{\overline{D}} \nabla \mathbf{U}_h^{n+1} \cdot \nabla \mathbf{v} dx = \\ \int_{\Omega} \left[\frac{4\mathbf{U}^n - \mathbf{U}^{n-1}}{2\tau_n} + \mathbf{F}^1(\mathbf{U}^n) - J_{\mathbf{F}^1}(\mathbf{U}^n) \mathbf{U}^n \right] \cdot \mathbf{v} dx \quad \forall \mathbf{v} \in Z_h. \end{aligned} \quad (4.5)$$

On the other hand, we seek $\mathbf{G}_h^{m+1} = (u_{4h}^{m+1}, u_{5h}^{m+1})^T$, for $0 \leq m \leq n$, such that

$$\frac{u_{4h}^{m+1} - u_{4h}^m}{\tau_m} = (1 - f_1) K_h u_{1h}^{m+1} + (1 - f_2) \frac{1 - Y}{Y} \left(\frac{u_{2h}^{m+1} - u_{2h}^m}{\tau_m} + K_d u_{2h}^{m+1} \right), \quad (4.6)$$

$$\frac{u_{5h}^{m+1} - u_{5h}^m}{\tau_m} = f_2 \frac{1 - Y}{Y} \left(\frac{u_{2h}^{m+1} - u_{2h}^m}{\tau_m} + K_d u_{2h}^{m+1} \right). \quad (4.7)$$

Remark 2. In our numerical simulations we choose $m = n$. Nevertheless, we write under this general form because it may be suitable for some applications to have two different time grids for the reaction-diffusion system and for the flow system.

4.2. Full discretization of the system (S2)

We discretize the equations (3.18) via the finite element method. The scheme consists to find $h_{ch}^{n+1} \in h_{c,D} + H_{1,h}$ and $h_{bh}^{n+1} \in h_{b,D} + H_{1,h}$ such that

$$\left\{ \begin{aligned} & \int_{\Omega} C_i(h_{ch}^n) \frac{h_{ch}^{n+1}}{\tau_n} \psi dx + \int_{\Omega} k_i(h_{ch}^n) (\nabla h_{bh}^{n+1} - \nabla h_{ch}^{n+1} - \mathbf{e}_z) \cdot \nabla \psi dx \\ & \qquad \qquad \qquad = \int_{\Omega} \rho^{-1} \alpha_{lh}^{n+1} \psi dx + \int_{\Omega} C_i(h_{ch}^n) \frac{h_{ch}^n}{\tau_n} \psi dx, \quad \forall \psi \in H_{0,h} \\ & \int_{\Omega} A_1(h_{ch}^n) \frac{h_{bh}^{n+1}}{\tau_n} \varphi dx - \int_{\Omega} A_2(h_{ch}^n, h_{bh}^n) \frac{h_{ch}^{n+1}}{\tau_n} \varphi dx \\ & \qquad \qquad \qquad + \int_{\Omega} \rho_b(h_{bh}^n) k_b(h_{ch}^n) (\nabla h_{bh}^{n+1} - \frac{\rho_b(h_{bh}^n)}{\rho_l} \mathbf{e}_z) \cdot \nabla \varphi dx \\ & \qquad \qquad \qquad = \int_{\Omega} \alpha_{bh}^{n+1} \varphi dx + \int_{\Omega} A_1(h_{ch}^n) \frac{h_{bh}^n}{\tau_n} \varphi dx \\ & \qquad \qquad \qquad + \int_{\Omega} A_2(h_{ch}^n, h_{bh}^n) \frac{h_{ch}^n}{\tau_n} \varphi dx \quad \forall \varphi \in H_{0,h} \end{aligned} \right. \quad (4.8)$$

5. Numerical results

In this section we present some numerical results for the problem (2.2)-(2.44). In all the experiments, we take $\Omega \subset \mathbb{R}^n$, $\partial\Omega = \Gamma_D \cup \Gamma_N$, with $n = 2$ for the 2D case and $n = 3$ for the 3D case as follows:

- $L = 10m$,
- for $n = 3$ (3D case), $\begin{cases} \Omega =]0, L[\times]0, L[\times]0, L[\\ \Gamma_D = \{(x, y, 0), \text{ with } (x, y) \in]0, L[\times]0, L[\} \end{cases}$
- for $n = 2$ (2D case), $\begin{cases} \Omega =]0, L[\times]0, L[\\ \Gamma_D = \{(x, 0), \text{ with } x \in]0, L[\} \end{cases}$

The different parameters used are given in TABLE (1) and TABLE (2) and come from [38] and [3]. From the same references, we take the initial conditions of the biodegradation system (in mgC/L) as indicated in TABLE (3).

The boundary conditions of the biodegradation system are all homogeneous Neumann conditions. The boundary and initial conditions for the flow system are given in TABLE (4).

We recall that at each time step, the system (2.2) is approximated by (4.4)-(4.7), and its solution gives the source terms of the two-phase flow system (2.44), approximated by (4.8). We note that some simulations of the 3D case are plotted with the software (Paraview) visualization tool.

Table 1. Parameters of the biodegradation.

$K_H(d^{-1})$	$\mu_m(d^{-1})$	f_1	f_2	$K_S(mgC/L)$	$K_d(d^{-1})$	Y	α	$K_I(mgC/L)$
0.176	0.3	0.7	0.76	160	0.04	0.05	0.9	10

Table 2. Parameters of the porous medium.

θ_r	θ_s	$K(m.s^{-1})$	$p_{ce}(m)$	b	$M_b(g/mol)$	$M_{H_2O}(g/mol)$	A_m
0.27	0.9715	10^{-4}	-0.0323	2.5	30	18.01	0.8
		$\mu_l(Kg.m^{-1}.s^{-1})$	$\mu_b(Kg.m^{-1}.s^{-1})$	$C_{Tb}(m^3/Kg)$			
		$4.61027 \cdot 10^{-4}$	10^{-5}	0.178			

Table 3. Initial conditions for the biodegradation system.

$X_0(x, y)$ (mgC/L)	$S_0(x, y)$ (mgC/L)	$[CO_2]_0(x, y)$ (mgC/L)	$[CH_4]_0(x, y)$ (mgC/L)
1751	0	0	0

Table 4. Initial and boundary conditions for the compressible two phase flow system.

$h_{c,0}(m)$ in Ω	$h_{b,0}(m)$ in Ω	$h_{c,D}(m)$ on Γ_D	$h_{b,D}(m)$ on Γ_D	$\mathbf{u}_l \cdot \mathbf{n}$ on Γ_N	$\mathbf{u}_b \cdot \mathbf{n}$ on Γ_N
$-1.3 \cdot 10^{-4}$	0	-0.0002	0	0	0

We recall that the landfill is considered to be an unsaturated and inhomogeneous porous medium due to a non-homogeneous distribution of the initial methanogenic bacteria B_0 as follows

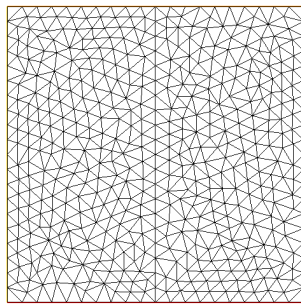
- In 2D:

$$B_0(x, z) = \begin{cases} 1 & \text{in } Z_1 := \{0 \leq x \leq L/2 \text{ and } 0 \leq z \leq L/2\}, \\ 2 & \text{in } Z_2 := \{L/2 \leq x \leq L \text{ and } 0 \leq z \leq L/2\}, \\ 3 & \text{in } Z_3 := \{0 \leq x \leq L \text{ and } L/2 < z < L\}. \end{cases}$$

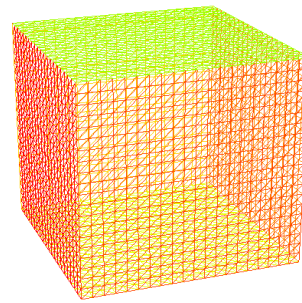
- In 3D:

$$B_0(x, y, z) = \begin{cases} 1 & \text{in } \Sigma_1 := \{0 \leq x \leq L/2, 0 \leq y \leq L \text{ and } 0 \leq z \leq L/2\}, \\ 2 & \text{in } \Sigma_2 := \{L/2 \leq x \leq L, 0 \leq y \leq L \text{ and } 0 \leq z \leq L/2\}, \\ 3 & \text{in } \Sigma_3 := \{0 \leq x \leq L, 0 < y < L \text{ and } L/2 \leq z < L\}. \end{cases}$$

We consider a quasi-uniform mesh of the domain Ω with (952 triangles and 517 vertices) in 2D and (48000 tetrahedras and 9261 vertices) in 3D (see FIGURE 3). We also consider $M_{bottom}(0.75L, 0.001L)$ a point at the bottom of the zone Z_3 , in which we will observe the evolution of leachate stagnation.



(a) 2D case



(b) 3D case

Figure 3. Mesh in 2D and 3D.

Taking into account the results obtained in [7] in terms of CPU computation time, we use partial (and not complete) diffusion. We then consider the diffusion $\bar{D} = \{D_X = 0.01, D_S = 0.03, D_B = 0.05\} [m^2/d]$. Using Haldane's law which is often more realistic, we obtain the following simulations.

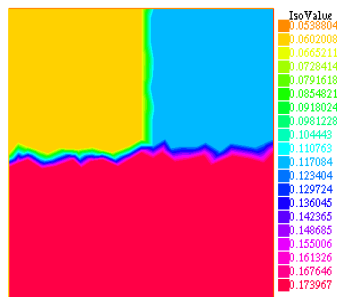
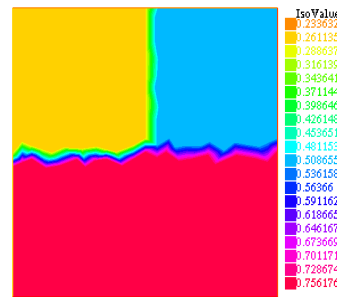
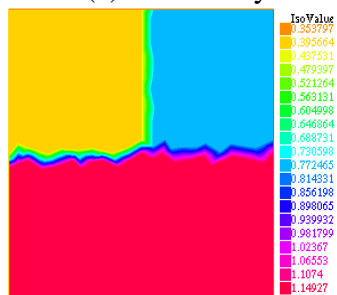
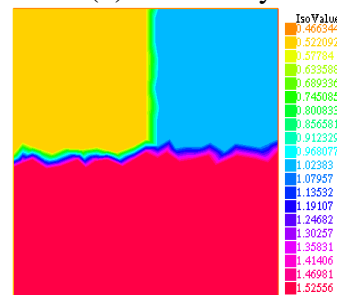
(a) $t = 0.1$ day(b) $t = 0.5$ day(c) $t = 1$ day(d) $t = 1.8$ day

Figure 4. Evolution of methane production in 2D.

Zones	t_1	t_2	t_3	t_4
Σ_1	Max=0.09 Min= 0.05	Max=0.39 Min= 0.23	Max=0.60 Min=0.35	Max=0.80 Min= 0.46
Σ_2	Max= 0.13 Min= 0.10	Max= 0.56 Min= 0.42	Max=0.85 Min=0.64	Max= 1.13 Min= 0.85
Σ_3	Max= 0.17 Min=0.14	Max= 0.75 Min=0.59	Max=1.15 Min=0.89	Max= 1.52 Min= 1.19

Table 5. Table of the Max and Min values of the methane production isovalues in the three zones over time according to the solutions obtained in Figure 4.

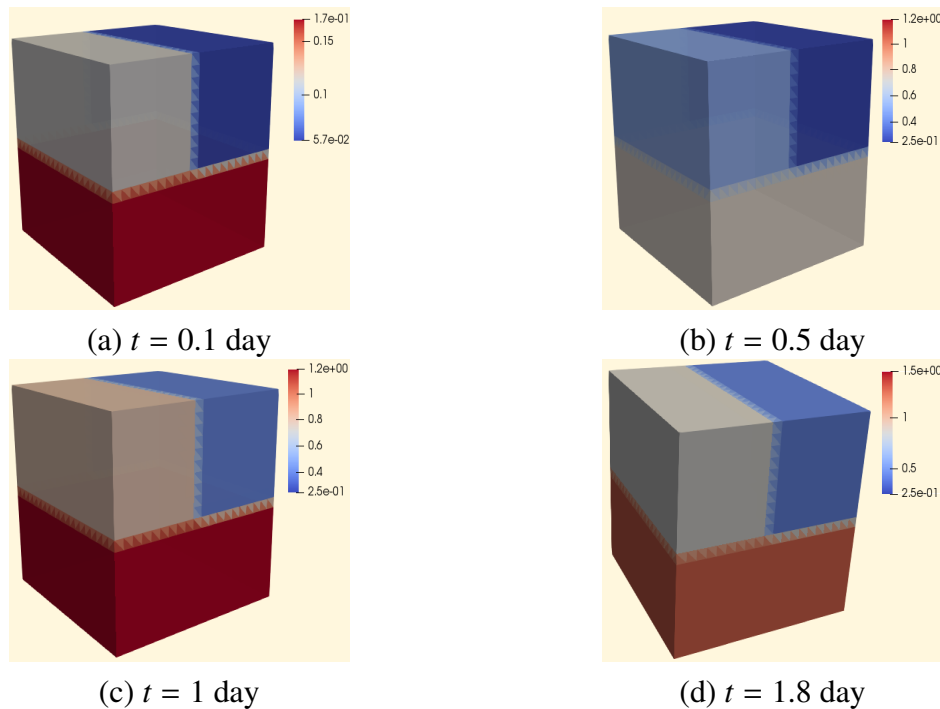


Figure 5. Evolution of methane production in 3D.

FIGURE 4 and FIGURE 5 show, respectively, the evolution of methane production in 2D and 3D at different times: $t_1 = 0.1$ day in (a), $t_2 = 0.5$ day in (b), $t_3 = 1$ day in (c) and $t_4 = 1.8$ day in (d).

From FIGURE 4, we notice that the the biogas production increases in the whole domain in proportion with the initial concentration of the methanogenic bacteria. More precisely, the mean value of the isovalues represented by "yellow color" goes from 0.06 at time t_1 to 0.52 at time t_4 , for the "blue color" region it goes from 0.12 at time t_1 to 1.02 at time t_4 , and the "red color" part from 0.17 at time t_1 to 1.52 at time t_4 . This agree with the results reported on Figure 6. In TABLE 5 we summarize the intervals of the isovalues for each region.

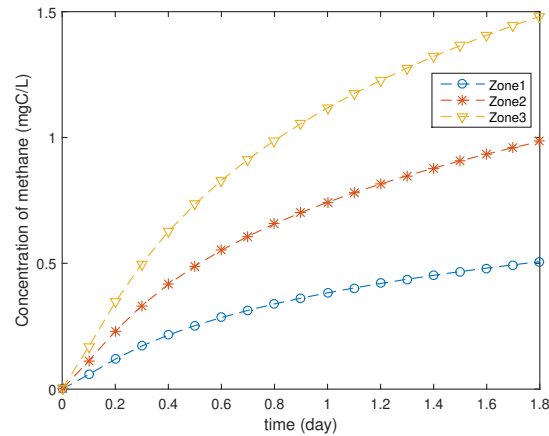


Figure 6. Evolution of the average methane production in each zone $\sum_i, i \in \{1, 2, 3\}$ (zone 1 corresponds to $B_0 = 1$, zone 2 corresponds to $B_0 = 2$ and zone 3 corresponds to $B_0 = 3$).

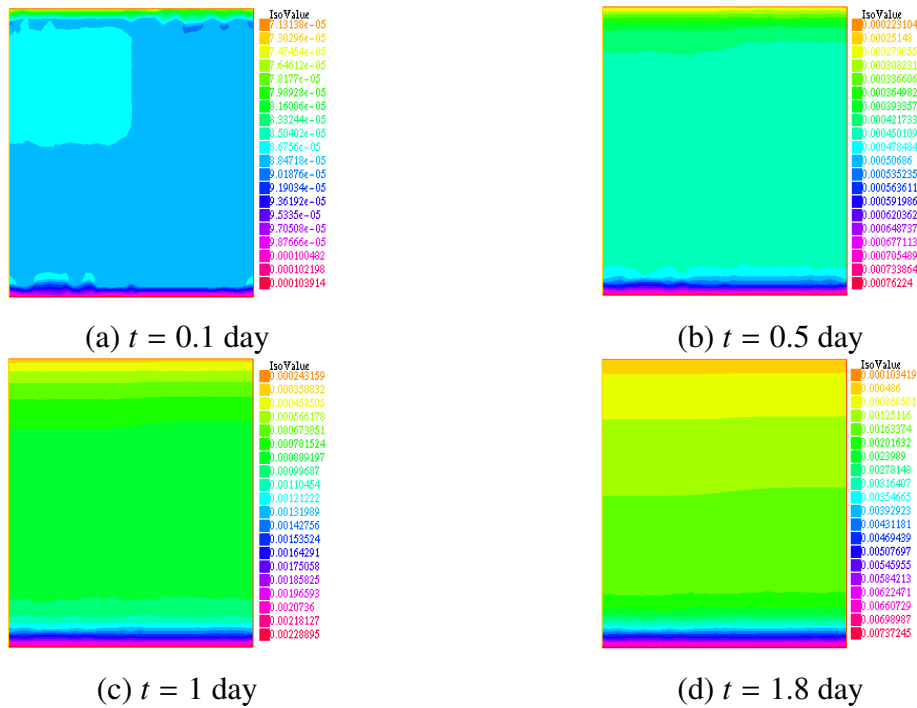


Figure 7. Evolution of the column height of biogas h_b in 2D.

Using the relationship between water content θ_l and capillary height h_c (see (2.15) and (2.20)), FIGURES 9 and 10 show the evolution of water content in 2D and 3D, respectively. Thus, we notice that the leachate starts to stagnate at the bottom of the domain at time t_4 . More precisely, FIGURE 11 shows the evolution of the water content at the point M_{bottom} in two-phase biogas-leachate flow case and one phase leachate flow case (see [7]). We notice that the yellow curve "two-phase flow case" indicates the increase of the water content over time, from the initial value $\theta_0 = 0.37$, to the value $\theta \approx \theta_s$ (value close to saturation), at time t_4 . Almost, the same situation of the start of leachate stagnation was

obtained at time $t = 2$ day in the case of single-phase leachate flow. Therefore, in the two-phase flow case and from the time t_4 , we will not have the biogas production in the small layer at the bottom of the domain because its water content value does not satisfy the condition of humidity for the biogas production.

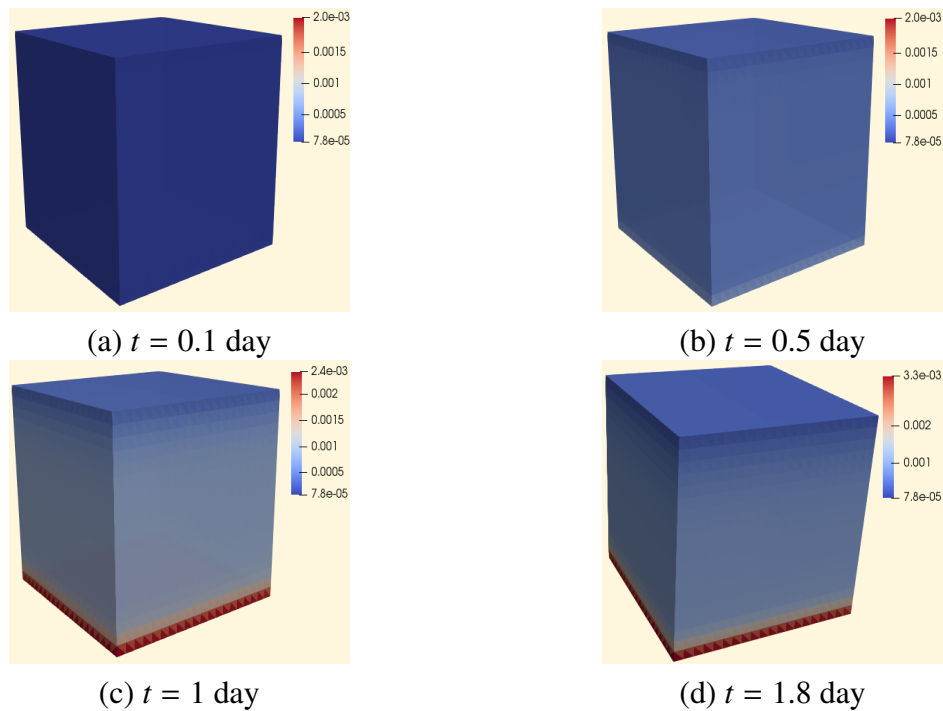


Figure 8. Evolution of the column height of biogas h_b in 3D.

FIGURE 7 and FIGURE 8 show respectively the evolution of the column height of the biogas h_b in 2D and 3D. We notice in FIGURE 7(a), which corresponds to time t_1 , the appearance of a sky blue colored area with very low values and which almost coincides with the zone where initially the concentration of the methanogenic bacteria is the lowest. The diffusion process yields a monotonically increasing biogas production and the pressure distribution becomes regular and spatially homogeneous (see the figures (b), (c) and (d) in FIGURE 7).

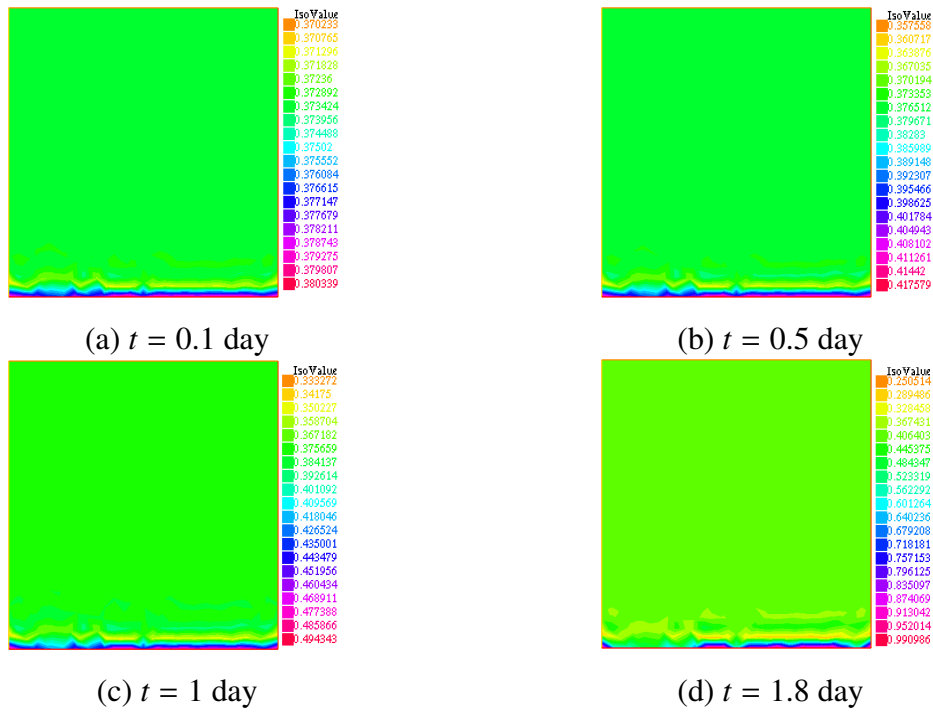


Figure 9. Evolution of the water content $\theta(h_c)$ in 2D.

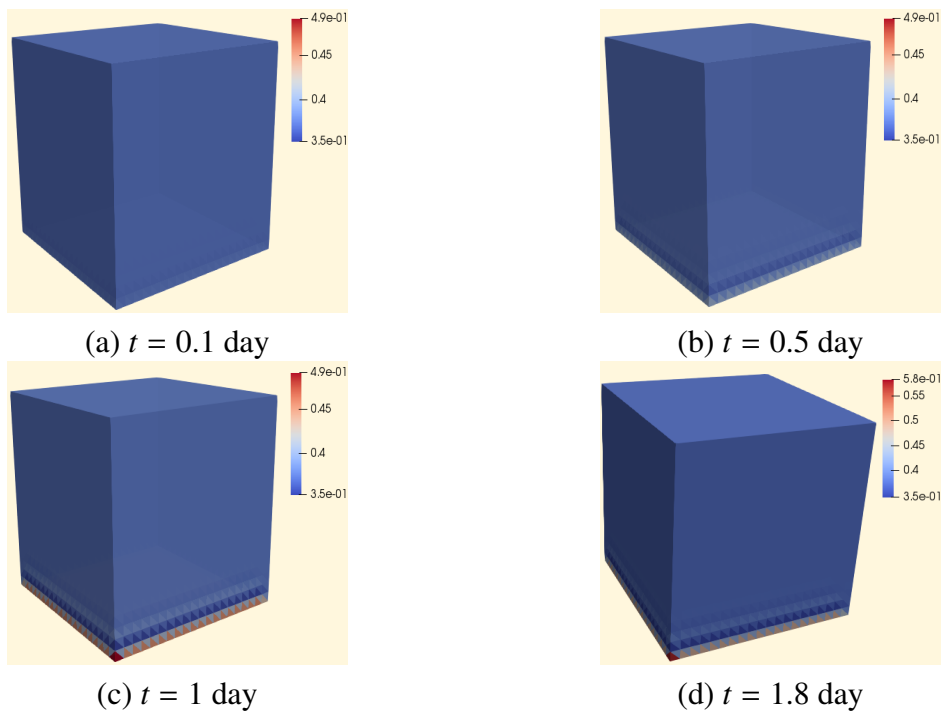


Figure 10. Evolution of the water content $\theta(h_c)$ in 3D.

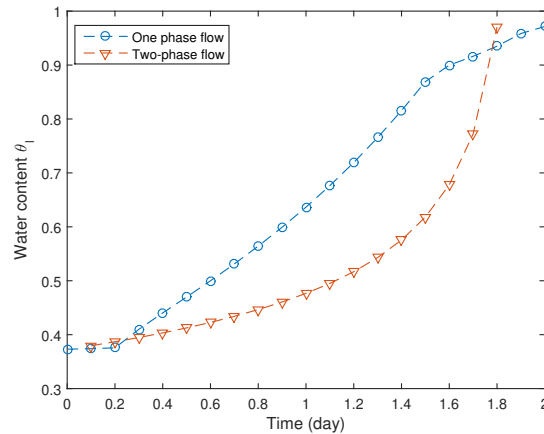


Figure 11. Evolution of the water content θ_l at the point M_{bottom} in one phase flow and two-phase flow problem.

The time t_4 corresponds approximately to the moment when a leachate stagnation zone will appear at the bottom of the landfill. The moisture condition necessary for the biogas production will not be satisfied in the whole area after this time, this gives a stopping criterion for the algorithm. Accordingly, for the waste landfill management and the energy production, one has to decide either to release the stagnant leachate or to inject to act on the humidity factor which means mathematically to fit the proposed model in the framework of an optimal control approach.

6. Conclusion

In this article, we have considered a new model describing the bacterial activity in a household waste landfill, taken as a reactive and unsaturated non-homogeneous porous medium. The coupling of the two-phase flow in the landfill and their interaction with the biological dynamic allows us to obtain accurately the leachate and the biogas. The outcome of the model, namely the pressure functions of these two phases are the key variables for the waste management and the energy production. The discrete setting which consists of a second order BDF2 time-scheme and finite elements approximation give an efficient discrete framework with respect to the accuracy and reasonable cost requirements. The computation code in 2D and 3D and the numerical simulations confirm the relevance of the model and the associated discrete setting. Finally, we notice that the impact of the humidity on the outcome appears to be important and the combination of the approach we developed in this article with an optimal control strategy may be a promising perspective.

Acknowledgments

The authors are gratefully for the French-Moroccan exchange program "PHC TOUBKAL 17/47".

Conflict of interest

The authors declare there is no conflict of interest.

References

1. F. AGOSTINI, C. SUNDBERG, R. NAVIA , *Is biodegradable waste a porous environment? A review.* Waste Management, Research, **30**(10)(2012), 1001-1015.
2. E. AHUSBORDE, B. AMAZIANE, M. EL OSSMANI, M. I. MOULAY , *Numerical Modeling and Simulation of Fully Coupled Processes of Reactive Multiphase Flow in Porous Media.* J. Math. Study, **52**(4)(2019), 359-377.
3. C. ARAN , *Modélisation des Ecoulements de Fluides et des Transferts de Chaleur au Sein des Déchets Ménagers. Application à la Réinjection de Lixiviats dans un Centre de Stockage.*(Ph.D. thesis)(2001), Institut National Polytechnique de Toulouse, France.
4. J. ARZATE, M. KIRSTEIN, F. ERTEM, E. KIELHORN, H. MALULE, P. NEUBAUER, M. CRUZ-BOURNAZOU, S. JUNNE , *Anaerobic digestion model (AM2) for the description of biogas processes at dynamic feedstock loading rates,* Chemie Ingenieur Technik, **89**(2017), 686–695.
5. M. AZAÏEZ, M. DEVILLE, E. H. MUND , *Éléments finis pour les fluides incompressibles.* PPUR Presses polytechniques (2011).
6. B. BENYAHIA, T. SARI, B. CHERKI, J. HARMAND , *Bifurcation and stability analysis of a two step model for monitoring anaerobic digestion processes.* Journal of Process Control, **22**(2012), 1008-1019.
7. Z. BELHACHMI, M. MGHAZLI, S. OUCHTOUT , *Mathematical modelling and numerical approximation of a leachate flow in the anaerobic biodegradation of waste in a landfill.* Mathematics and Computers in Simulation, 185 (2021), 174-193.
8. G. BELLENFANT , *Modélisation de la production de lixiviat en centre de stockage de déchets ménagers.* (Doctoral dissertation, Institut National Polytechnique de Lorraine-INPL)(2001).
9. O. BERNARD, Z. HADJ-SADOK, D. DOCHAIN, A. GENOVESI, J. P. STEYER , *Dynamical model development and parameter identification for an anaerobic wastewater treatment process.* Biotechnology and bioengineering, **75**(4)(2001), 424-438.
10. D. BOTHE, A. FISCHER, M. PIERRE, G. ROLLAND , *Global wellposedness for a class of reaction-advection-anisotropic-diffusion systems.* Journal of Evolution Equations, **17**(1)(2017), 101-130.
11. R.H. BROOKS, A.T. COREY, *Hydraulic Properties of Porous Media,* Colorado State Univ. Hydrology Paper No. 3(1964), 27 pp.
12. G. S. CAMPBELL, *A simple method for determining unsaturated conductivity from moisture retention data.* Soil science, **117**(6)(1974), 311-314.
13. Z. CHEN, G. HUAN, Y. MA , *Computational methods for multiphase flows in porous media (Vol. 2).* Siam (2006).
14. D. CHENU , *Modélisation des transferts réactifs de masse et de chaleur dans les installations de stockage de déchets ménagers: application aux installations de type bioréacteur.* (Doctoral dissertation, Institut National Polytechnique de Toulouse) (2007).
15. I. DIDI, H. DIB, B. CHERKI , *A Luenberger-type observer for the AM2 model,* Journal of Process Control, **32**(2015), 117-126.

16. N. DIMITROVA, M. KRASTANOV , *Model-based optimization of biogas production in an anaerobic biodegradation process*, Computers and Mathematics with Applications, vol. **68**(2014), no 9 : 986-993.
17. G. DOLLÉ, O. DURAN, N. FEYEU, E. FRÉNO, M. GIACOMINI, C. PRUD'HOMME , *Mathematical modeling and numerical simulation of a bioreactor landfill using Feel++*. ESAIM: Proceedings and Surveys, **55**(2016), 83-110.
18. M. EL HAJI, F. MAZENC, J. HARMAND , *A mathematical study of a syntrophic relationship of a model of anaerobic digestion process*. Mathematical Biosciences and Engineering, **7**(3)(2010), 641.
19. R. FEKIH-SALEM, J. HARMAND, C. LOBRY, A. RAPAPORT, T. SARI , *Extensions of the chemostat model with flocculation*. Journal of Mathematical Analysis and Applications, **397**(2013), 292–306.
20. M. GABBOUHY, Z. MGHAZLI , *Un résultat d'existence de solution faible d'un système parabolique-elliptique non linéaire doublement dégénéré*. In Annales de la Faculté des sciences de Toulouse: Mathématiques (Vol. **10**, No. 3(2001), pp. 533-546).
21. C. GALLO, G. MANZINI , *A fully coupled numerical model for two-phase flow with contaminant transport and biodegradation kinetics*. Communications in Numerical Methods in Engineering, **17**(5)(2001), 325-336.
22. S. GHOLAMIFARD , *Modélisation des écoulements diphasiques bioactifs dans les installations de stockage de déchets*. (Doctoral dissertation, Université Paris-Est)(2009).
23. J. HARMAND, C. LOBRY, A. RAPAPORT, T. SARI , *The Chemostat: Mathematical Theory of Microorganisms Cultures*, ISTE Wiley (2017).
24. S. HASSAM, E. FICARA, A. LEVA, J. HARMAND , *A generic and systematic procedure to derive a simplified model from the anaerobic digestion model*, No. 1 (ADM1), Biochemical Engineering Journal, **99**(2015), 193–203.
25. F. HECHT, "New development in FreeFem++." Journal of numerical mathematics 20.3-4 (2012): 251-266.
26. R. HELMIG , *Multiphase flow and transport processes in the subsurface: a contribution to the modeling of hydrosystems*. Springer-Verlag (1997).
27. F. HÉNON, G. DEBENEST, X. LEFEVRE, S. POMMIER, D. CHENU, M. QUINTARD , *Simulation of Transport and Impact of Moisture Content on the Biodegradation*. Fourth International Workshop "Hydro-Physico-Mechanics of Landfills", Santander, Spain (2011).
28. M. HMISSI, J. HARMAND, V. ALCARAZ-GONZALEZ, H. SHAYEB , *Evaluation of alkalinity spatial distribution in an up-flow fixed bed anaerobic digester*, Water Science and Technology, **77**(2018), 948–959.
29. P. C. LICHTNER , *Continuum formulation of multicomponent-multiphase reactive transport*. Reviews in mineralogy, **34**(1996), 1-82.
30. J. KINDLEIN, D. DINKLER, H. AHRENS , *Numerical modelling of multiphase flow and transport processes in landfills*. Waste Management and Research, **24**(4)(2006), 376-387.
31. S. LANINI, *Analyse et modélisation des transferts de masse et de chaleur au sein des décharges d'ordures ménagères*. (Doctoral dissertation, Institut National Polytechnique de Toulouse)(1998).

32. D. NGUYEN-NGOC, B. LEYE, O. MONGA, P. GARNIER, N. NUNAN , *Modeling microbial decomposition in real 3D soil structures using partial differential equations*. International Journal of geosciences, **4**(10)(2013), 15.
33. S. OUCHTOUT, Z. MGHAZLI, J. HARMAND, A. RAPAPORT, Z. BELHACHMI, *Analysis of an anaerobic digestion model in landfill with mortality term*, Communications on Pure and Applied Analysis, vol. **19**, no 4 (2020): 2333.
34. G. F. PINDER, W. G. GRAY , *Essentials of multiphase flow and transport in porous media*. John Wiley and Sons (2008).
35. F.G. POHLAND, B. AL-YOUSFI , *Design and Operation of Landfills for optimum stabilization and biogaz production*. Wat. Sci. Tech., Vol.**30**, no 12(1994), pp.117-124.
36. A. RAPAPORT, T. NIDELET, S. EL AIDA, J. HARMAND , *About biomass overyielding of mixed cultures in batch processes*, Mathematical biosciences, vol. **322** (2020), p. 108322.
37. A. RAPAPORT, T. NIDELET, J. HARMAND , *About biomass overyielding of mixed cultures in batch processes*, in 8th IFAC Conference on Foundations of Systems Biology in Engineering (FOSBE), Valencia, Spain, 15-18 Oct., (2019).
38. M. ROUEZ , *Dégradation anaérobie de déchets solides: Caractérisation, facteurs d'influence et modélisations*. Laboratoire de Génie Civil et d'Ingénierie Environnementale. Lyon, Institut National des Sciences Appliquées Docteur, 259 (2008).
39. J. SHI, Y. WU, X. ZOU , *Coexistence of Competing Species for Intermediate Dispersal Rates in a Reaction–Diffusion Chemostat Model*. Journal of Dynamics and Differential Equations **32**(2) (2020): 1085-1112.
40. H. L. SMITH, P. WALTMAN , *The theory of the chemostat: dynamics of microbial competition (Vol. 13)*. Cambridge university press (1995).
41. M. T. VAN GENUCHTEN , *A closed-form equation for predicting the hydraulic conductivity of unsaturated soils I*. Soil science society of America journal, **44**(5)(1980), 892-898.
42. P. A. VANROLLEGHEM, D. DOCHAIN , *Dynamical Modelling and Estimation in Wastewater Treatment Processes*. IWA Publishing, 2001.